Supplementary Information for

Pulsed Electron Paramagnetic Resonance on two Cu(II)-Cage Compounds With Six, Respectively Eight Copper Ions

Leonardo Passerini[1], Eduard O. Bobylev[2], Felix J. De Zwart[2], Henrik Hintz[3], Adelheid Godt[3], Bas de Bruin[2], Joost Reek[2], Martina Huber[2]

[1]Department of Physics, Leiden University, the Netherlands Huygens-Kamerlingh Onnes Laboratory, Molecular Nano Optics and Spins, Leiden, 2333 CA, the Netherlands.

[2]Van't Hoff institute for molecular sciences, University of Amsterdam, Amsterdam, 1090 GD, the Netherlands.

[3]Department of Chemistry, Bielefeld University, Bielefeld, D-33615, Germany

Spplementary text

Meaning of geometric interpretation, Cu8: cube, Cu6: octahedron

The description of the arrangement of the Cu-ions in the cages as a cube (**Cu8**) or an octahedron (**Cu6**) facilitates the description of the arrangement of the Cu-ions, but does not imply that the ions form an idealized geometric body. The uncertainty range for the distances obtained from the models (Table 1, main text) gives the range of distances of individual pairs of Cu-ions. In an ideal cube or octahedron all distances between the specific types of Cu-ions should be identical. However, especially the model 2 structures show clear deviations from the shapes, as seen in figure SI1, where the distortions already can be seen in the figure.

The corners of polyhedra also have specific relations between distances: In a cube, the relation between the shortest distance (distance ***a***) along the edge of the cube and the face-diagonal (distance ***b***) is $\boldsymbol{b} = 1/\sqrt{2}\ \boldsymbol{a}$, the same as the ratio between the shorter and the longer distance in an octahedron. As a result, the distances in **Cu6** and **Cu8** are expected to follow this ratio.

Overview of measurement

The DEER traces presented here can be compared to those shown in Bobylev *et al.* [1]. For **Cu6**, increasing the accumulation time and optimizing the pulse-excitation resulted in a better signal-to-noise ratio, increasing the confidence level for the distance-distribution shape compared to the traces shown in figure 8 and 10 of [1], while leading to the same distances as before. For **Cu8**, several attempts to improve the signal-to-noise ratio in a similar way did not improve the data due to a combination of factors, suggesting that the shorter T_m time or other chemical factors cause the lower signal-to-noise ratio compared to what can be achieved for **Cu6**. In [1] DEER was one of several methods to verify the structure of the cages, so the focus was on the distances only. In the present manuscript, the number of interacting spins is determined by a direct comparison with a two-copper model compound (**Cu2**) enabling detailed analysis of this point in the multi-copper systems investigated. Additionally several different analysis methods were applied (Gaussian analysis of DEER traces, and DeerNet), see below, to quantitate the reliability of the analysis. Most of the differences observed with respect to [1], such as that the second distance peak in the **Cu8** distance distribution centered at 2.6 nm, see figure 2, is reliable, result in a higher confidence in the interpretation and are due to the better signal to noise ratio of the data.

Reproducibility was checked by measuring samples multiple times, and also measuring samples that had not been measured before. In between measurements, the EPR tubes with the samples were stored in liquid nitrogen, and introduced into the precooled resonator, to avoid accidental warming of the samples as much as possible.

Possible orientation-selection effects in the DEER traces

As mentioned in the main text, orientation-selection effects can lead to a reduction of the copper-copper interaction observed by DEER, which reduces the modulation depth, i.e. the total number of spins interacting (see discussion main text). Also, orientation selection can affect specific pairs of spins more strongly than others, which would cause a deviation of the relative intensity of the distance peaks from the expected intensities given in table 1, main text. In the DEER experiments, both the pump- and the observer frequencies were positioned in the perpendicular region of the EPR spectrum, see figure 2 main text and figure SI3. Therefore, spin pairs in which the parallel component, i.e. g_{zz}, of the g-tensor of one Cu(II) is parallel to the perpendicular component, i.e. the g_{xx}-g_{yy} plane, of the other Cu(II) will not contribute to the DEER effect, because for these pairs only one of the two partners are excited. The actual orientation of g-tensors of pair could also be in between the extremes, leading to partial excitation of a pair, for example. Consequently, the relative orientation of the g-tensors of two coppers in the cages determines how much these two Cu(II) centers contribute to the DEER effect. This can lead to reduced or absent DEER effects for specific pairs. As the g-tensor directions of the Cu(II)-centers in the Cu-cages are not known, the contribution of this effect cannot be estimated. Experimentally, orientation effects can be determined by setting the pump-pulse to a parallel and the observer pulse to a perpendicular position in the EPR spectrum, and vice versa, however, for Cu(II), the limited bandwidth of the resonator does not allow this. Other approaches have been used as well, see [3-6], however, in the present case, the sensitivity was not sufficient to measure meaningful DEER traces in the parallel region of the spectrum, as would be needed to use such an approach. Thus, orientation-selection effects can effectively lower the number of spins observed, and can lead to a difference in the relative intensity of distance peaks from those expected, see below.

Applying different analysis methods for DEER data

Different analysis methods for the DEER data were tested to (i) determine the reliability of the analysis described in the main text and (ii) to investigate if other interpretations are compatible with the data.

(i) The DeerNet analysis (figure SI 9 and 10) shows that also the shape of the distance distribution is robust and agrees with the Tikhonov analysis, as confidence levels and shape agree. For using DeerNet, unfortunately, the signal-to-noise ratio (12 for **Cu6** and 9 for **Cu8**) is at or below the limit of the S/N-ratio recommended in DeerNet. So in this case, the advantage of the DeerNet program, namely that processing of baseline and form factor is user-invention free [7, 8], cannot be fully harnessed: The simulated form-factor contribution, especially for **Cu8**, figure SI 10A, is less smooth than we would chose. The DEERNet option to do Tikhonov analysis shown in Fig. SI 9B and 10B can be directly compared to that in Fig. 2B, main text, showing that a smaller regularization parameter selected in the user-adjusted Tikhonov regularization smoothens out some of the features that we interpret as noise. So we see that in this very specific case, while DeerNet confirms the overall distance distribution, and unambigously quantifies trace parameters such as the signal-to-noise ratio, it cannot be used as the only method of data analysis.

(ii) Analysis of the data with Gaussian distance distributions enables to change distance parameters, such as center-distance and -width of the distance peaks individually. Here we checked if the distance peaks could have different widths, however, as figure SI7 and SI8 show, the optimum solution is similar to the Tikhonov one.

Also, we tested if different relative weights of the distance peaks were compatible with the data, given that the expected intensity of the distance peaks (see Tab. 1, main text) deviates from those found in Tikhonov analysis.

We found that for **Cu6**, changing the weight by more than 25 %, maintaining the width constant, results in significant deviation from the experimental DEER curve (data not shown), revealing that the deviation of the relative weights of the respective distances from the expected intensity ratios of the distance peaks (table 1, main text) is outside the experimental uncertainty. In the case of **Cu8**, also simulating with two Gaussian distance peaks is possible, (data not shown), probably attributable to the intrinsically low population of the third distance peak at 3.4 nm. For these tests, the distance and the width of the distance peaks were kept within a narrow range, so it cannot be excluded that larger variations of the relative weights of the distance peaks would be possible if the other parameters are changed more extensively. Due to the overall low signal-to-noise ratio of the data we did not expect unambiguous solutions.

Modulation depth and the relative intensities of the distance peaks

Deviations of the intensity of the distance peaks (figure 2, main text) from the expected intensities (Table 1 main text) can be due to incomplete ghost-peak supression in multispin systems as described in the main text. Specific factors can also enter: For **Cu6**, instead of the expected ratios of 4:1 (1.8 nm relative to 2.6 nm peak, figure 2) the distance peak at 1.8 nm is somehwat broadened, but not four times more intense than the distance peak at 2.6 nm. One reason could be a less favorable orientation selection for the Cu-pairs at the shorter distance, resulting in a smaller probability to excite just these pairs, and thereby causing lower intensity of the specific distance peak, see above. Also, the model predicts that the distance between some Cu-pairs may be as short as 1.5 nm. For such short distances, the excitation bandwidth of the pulses would not be sufficient, resulting in a smaller contribution of these distances, and thereby, again, a smaller intensity for the distance peak at 1.8 nm. We tested this with the limited-bandwidth-excitation feature in DeerAnalysis but found only small changes, so it is probably not the main factor contributing. For **Cu8**, similar arguments than for **Cu6** can be made. In addition, the overall broader lines in the distance distribution could be an indication that, as seen in model 2, multiple conformations contribute and that the superposition of those conformations of the cage smear out the distance peaks.

Why not all spins in the cages are observed

Several factors contribute to the uncertainty of the number of interacting spins determined: Measurement and interpretation of the modulation depth requires that sample and reference are measured with precisely the same conditions. Therefore, measurements were performed in the same experimental run, to minimize day to day variations, and with shorter evolution times to improve signal-to-noise ratios. Also, the spectra of sample and reference must have similar anisotropies. As figure SI3 shows, the EPR spectra of the Cu-cages and the reference compound almost overlap, showing that this condition is fulfilled. Several other factors, such as orientation selection (see above) and partial reduction the Cu-ions in the cages [1] , can lead to a smaller number of spins measured than expected. Another factor that can reduce modulation depth is a contribution of short distances, since for short distances, the excitation bandwidth of the pulses is not sufficient to excite the dipolar interaction. As a result, pairs at very short distances, roughly below 1.6 nm at our experimental conditions, would contribute less, or not at all to the modulation depth. This may contribute here, as the DEER time traces (figure 2, main text) show a fast initial decay, suggesting a contribution of spin-pairs at short distances, and, for **Cu6**, the models show distances can be as short as 1.5 nm. Also, orientation selection, described above, can cause specific pairs of spins to contribute less to the modulation depth than others. As several of the factors described reduce the modulation depth, the measured value should be considered as a lower limit.

Supplementary figures

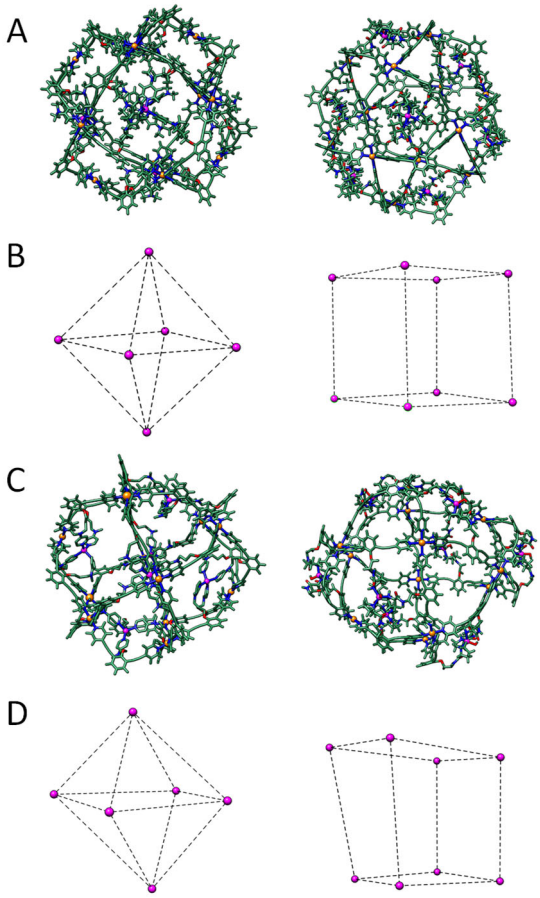

Figure SI.1. Model structures of copper cages. A) Model 1 structures. B) Relative position of the copper ions in model 1. C) Model 2 structures. D) relative position of the copper ions in model 2. Left: **Cu6**, right: **Cu8**. Orange: Palladium, Magenta: Copper ions. See main text and Bobylev *et al.* [1].

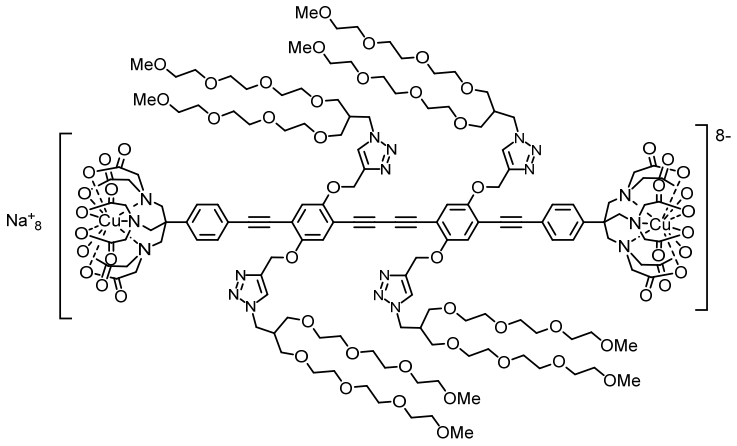

Figure SI.2. Structure of **Cu2**, used as a two copper reference. For details, see main text.

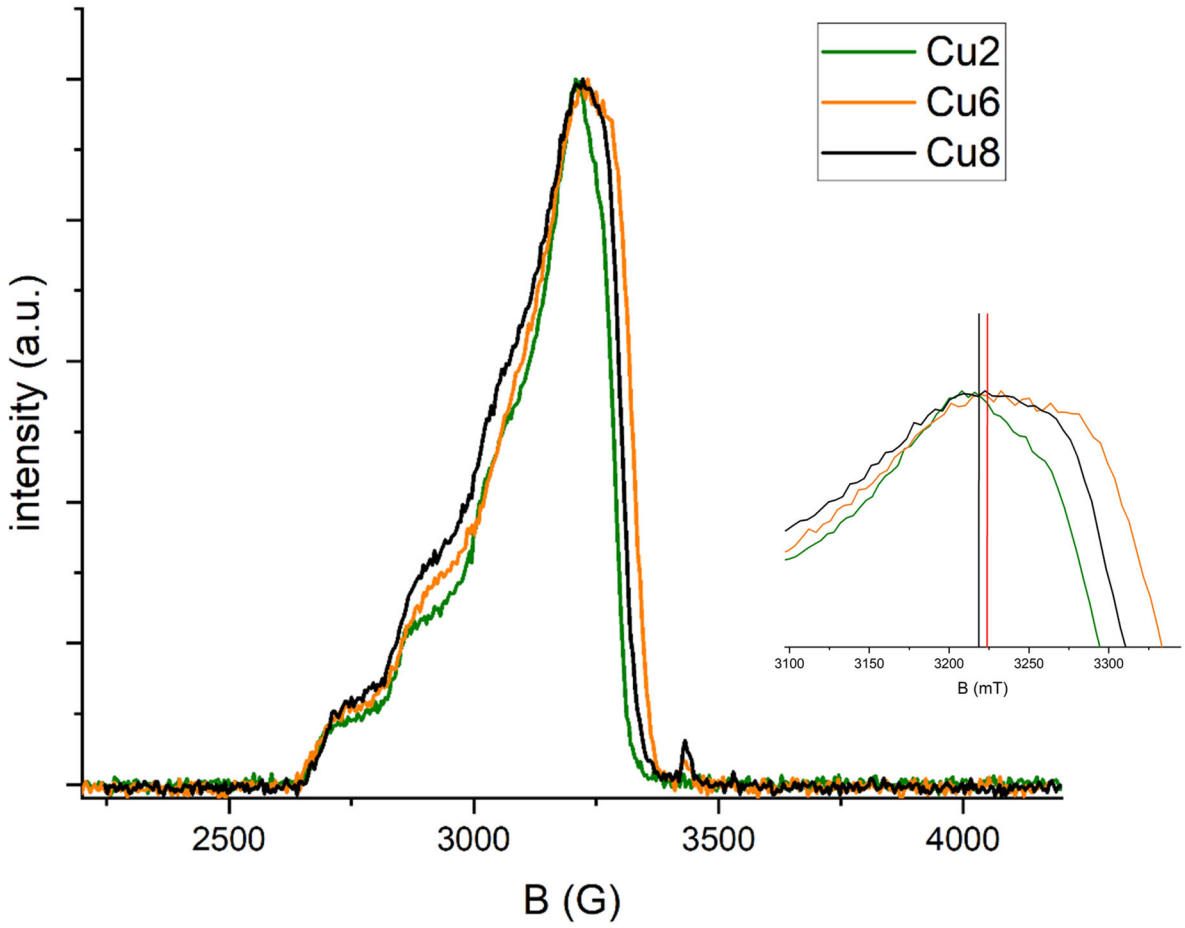

Figure SI.3. Field swept echo detected EPR spectra of all compounds. Green: **Cu2**, orange: **Cu6**, black: **Cu8**. Spectra were baseline corrected and normalized to maximum intensity. Overall similarity of spectra suggests that excitation in DEER is similar, but differences in orientation selection cannot be excluded (see text). The lines in the inset indicate position of the pump (red) and observer (black) pulses.

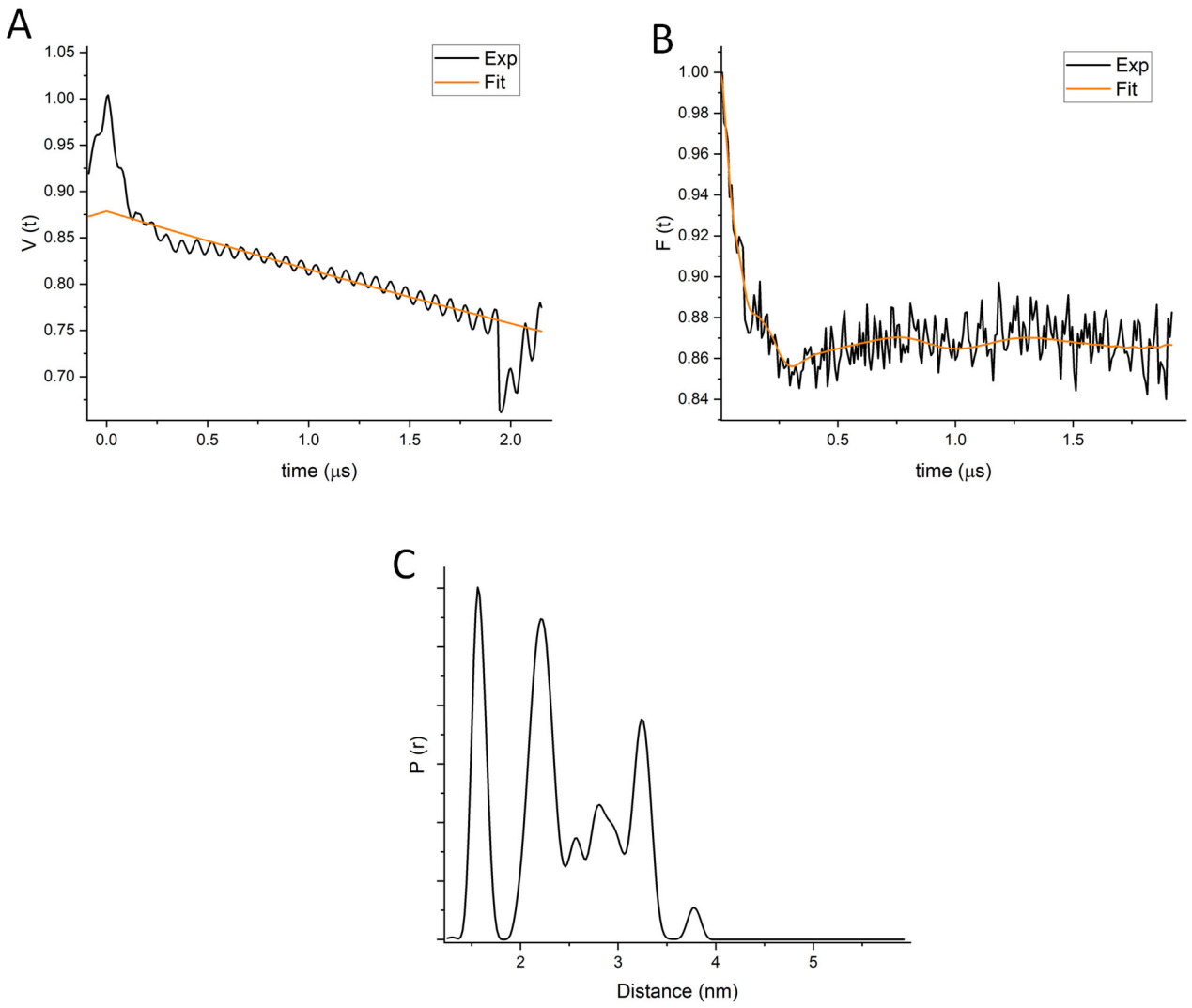

Figure SI.4. Results of DEER experiments with **Cu2**. A) Raw DEER trace (black) background (orange). B) Background subtracted DEER trace (black) with fit (orange). Maximum echo intensity (A,B) is normalized to unity. V(t) : primary measured data, normalized to maximum intensity. F(t) : form factor obtained after background subtraction. For details and experimental parameters, see text. C) Distance distribution obtained for **Cu2:** expected distance is 3.3 nm. It was shown in Keller *et al.* [2] that several peaks of the distance distribution derive from contributions of weak exchange-coupling, for which we do not correct here. Peak at 1.5 nm: possible artifact for non-completely suppressed proton modulation.

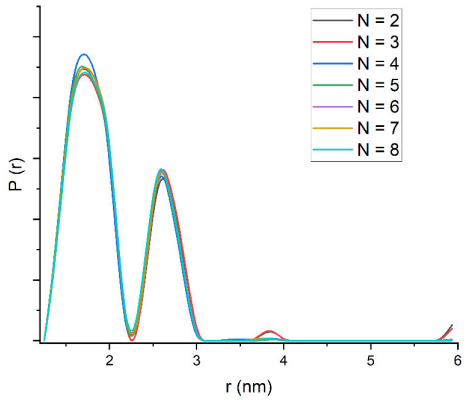

Figure SI.5. Effect of ghost suppression on **Cu8** distance distribution, from N = 2 to to N = 8, eight interacting Cu(II). For details, see Materials and Methods section and main text.

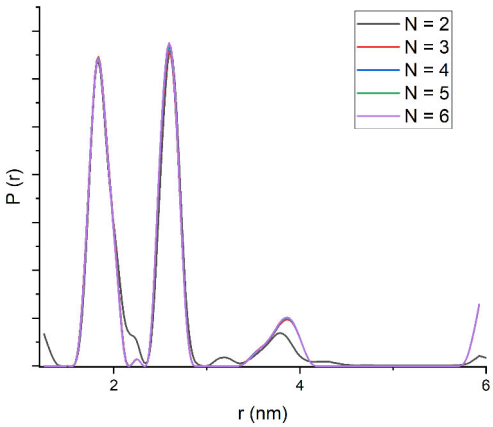

Figure SI.6. Effect of ghost suppression on **Cu6** distance distribution, from N = 2 to N = 6. For details, see Materials and Methods section and main text.

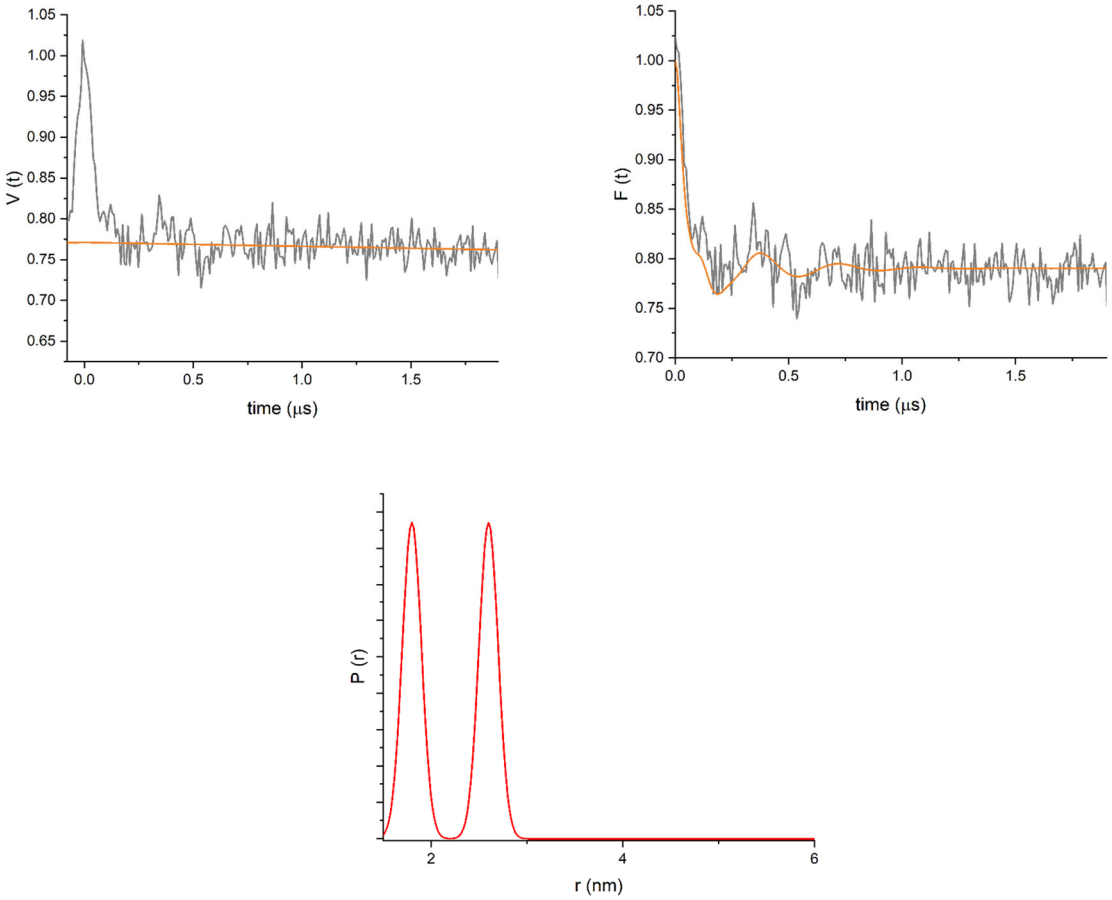

Figure SI.7. **Cu6** data analyzed with two-Gaussian fitting in DeerAnalysis. DEER trace (grey) and background (orange), background subtracted trace (grey) and fit (orange), distance distribution. N=2 spins, and two Gaussian peaks centered at 1.8 and 2.6 nm. Manually changing the width or center of the Gaussians did not significally improve the agreement with the data. For details, see text.

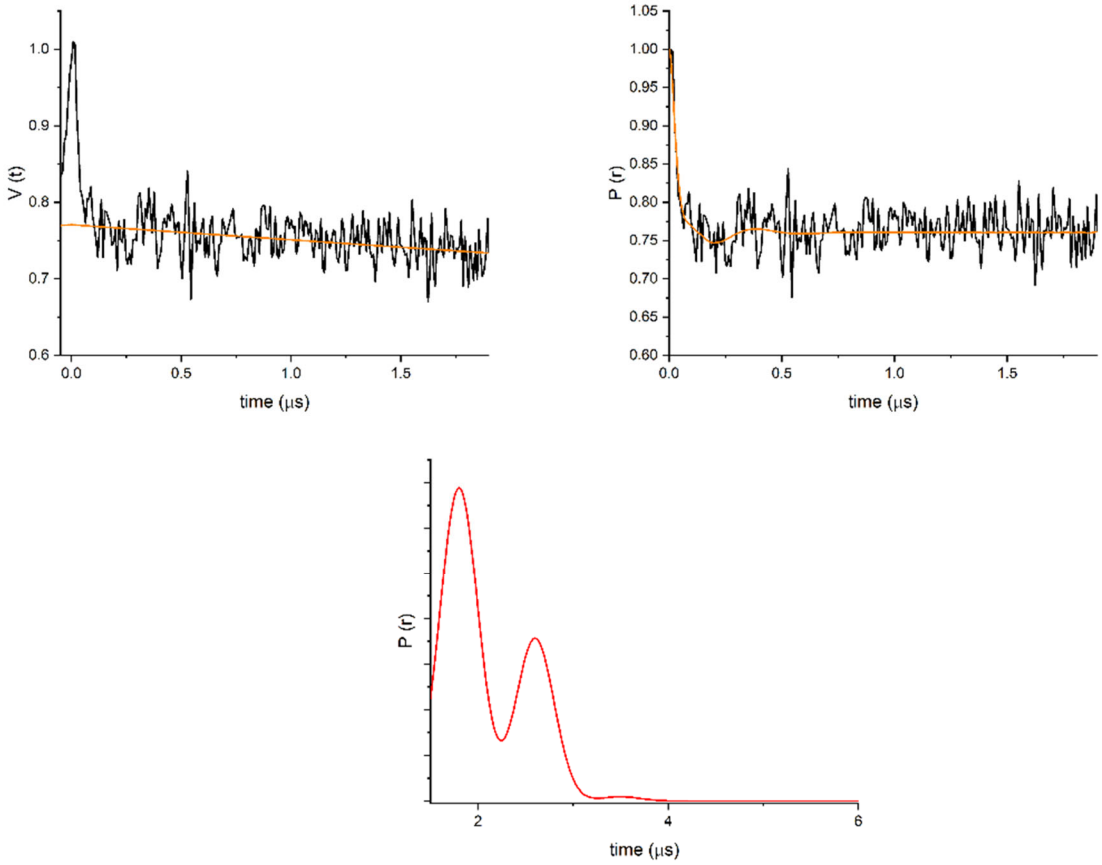

Figure SI.8. **Cu8** data analyzed with three-Gaussian fitting in DeerAnalysis. DEER trace (black) and background (orange), background subtracted trace (black) and fit (orange), distance distribution. N=2 spins, and three Gaussian peaks centered at 1.8, 2.6 and 3.5 nm. Manually changing the width or center of the Gaussians did not significally improve the agreement with the data. For details, see text.

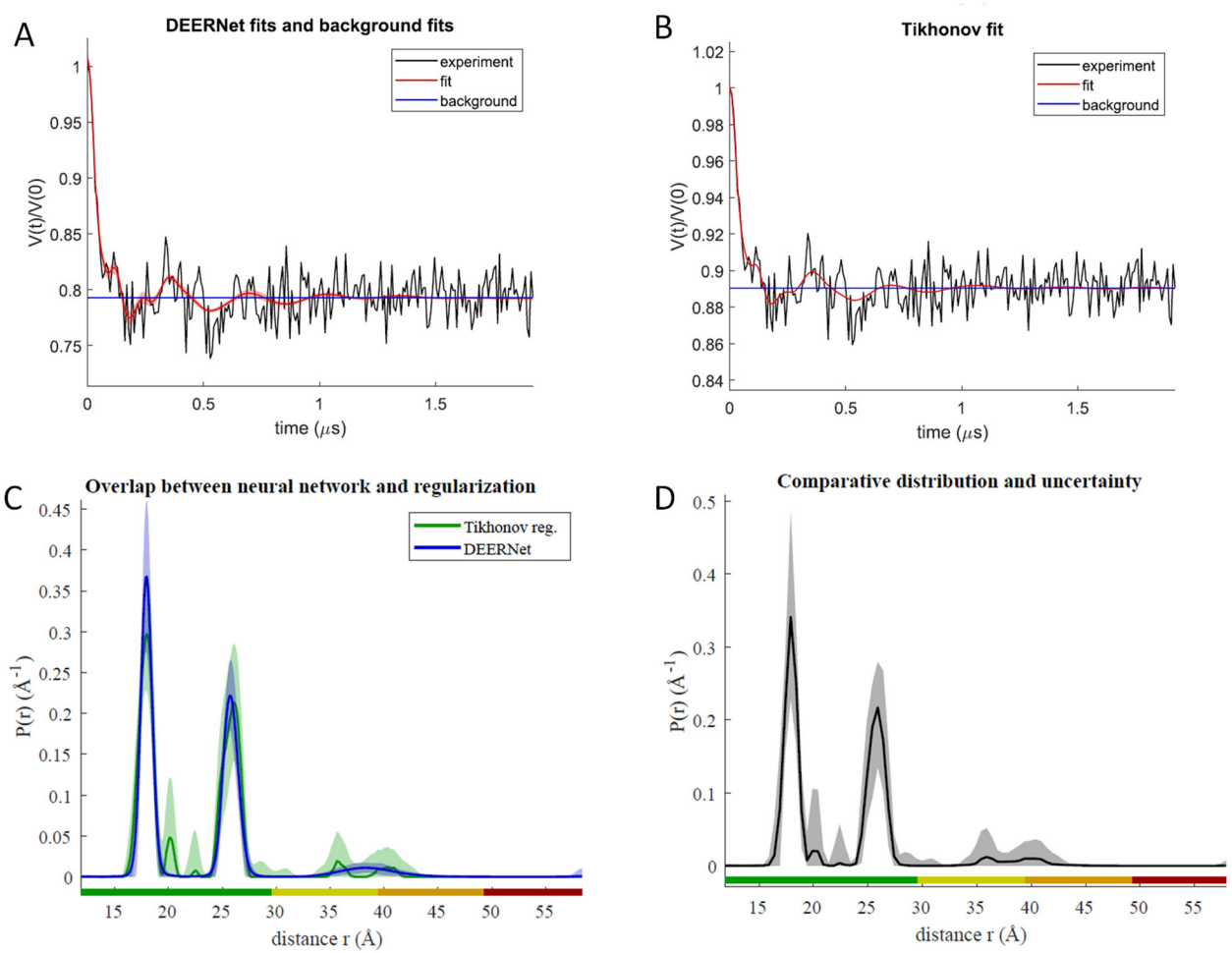

Figure SI.9. **Cu6** data analyzed with DEERNet tool in DeerAnalysis 2023. A) Deer trace (black), background (blue), fit (red) from DEERNet. B) Deer trace (black), background (blue), fit (red) from Tikhonov regularization. C) distance distribution, comparison between DEERNet (blue) and Tikhonov regularization (green). D) Comparative distribution from C). Shaded area in C) and D): uncertainty margins. The colors on the abscissa axis of the distance distribution indicate reliability of distance peaks: green: shape of distance distribution is reliable, yellow: mean distance and width are reliable, orange: mean distance is reliable, red: distance may be detectable, but cannot be quantified. Compared to the Tikhonov results shown in the main text (Figure 2), the regularization parameters is larger, which we consider an over-interpretation of the data.

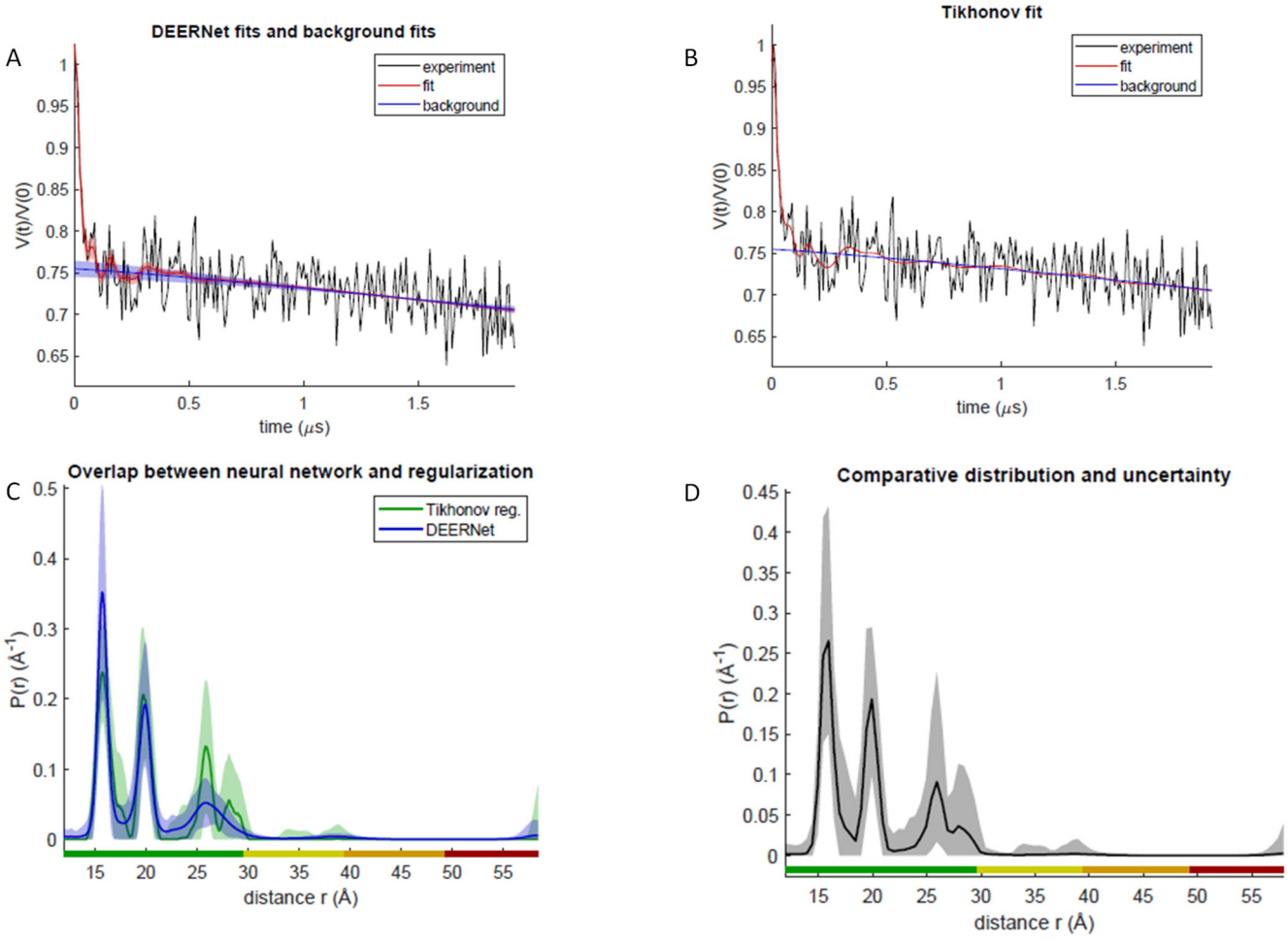

Figure SI.10. **Cu8** data analyzed with DEERNet tool in DeerAnalysis 2023. A) Deer trace (black), background (blue), fit (red) from DEERNet. B) Deer trace (black), background (blue), fit (red) from Tikhonov regularization. C) distance distribution, comparison between DEERNet (blue) and Tikhonov regularization (green). D) Comparative distribution from C). Shaded area in C) and D): uncertainty margins. The colors on the abscissa axis of the distance distribution indicate reliability of distance peaks: green: shape of distance distribution is reliable, yellow: mean distance and width are reliable, orange: mean distance is reliable, red: distance may be detectable, but cannot be quantified. Overall, DEERNET confirms results presented in main text. In contrast to the Tikhonov results shown in figure 2 (main text), the main peak at 1.7 nm is split into two peaks (1.6 and 2.0 nm), however, the data are at the lower end of the recommened signal to noise ratio for DeerNet. Compared to the Tikhonov results shown in the main text, the regularization parameters is larger, which we consider an over-interpretation of the data. Overall, DEERNet confirms results presented in main text.

Table SI 1 Measured relaxation time constants for the cages **Cu6** and **Cu8**. T_m: phase-memory time. T_1: spin-lattice-relaxation time. The T_m relaxation was measured with the two-pulse sequence (π/2)-τ- (π)- τ-[echo] with an initial τ of 200 ns and 4 ns step increments. The T_1 relaxation was measured with the inversion-recovery sequence (π)- T-(π/2)-τ- (π)- τ-[echo]. The τ value was kept constant at 200 ns, starting T value was 400 ns with 40 ns step increments. 16 ns length for π/2 pulses and 32ns for π pulses were used. The T_m and T_1 time constants were obtained through exponential fitting. Measurement temperature: 30K.

	Cu6	**Cu8**
T_m (ns)	**522 ± 11**	**302 ± 7**
T_1 (µs)	**8.7 ± 0.4**	**15.4 ± 0.5**

References

[1] E.O. Bobylev, L. Passerini, F.J. de Zwart, D.A. Poole, S. Mathew, M. Huber, B. de Bruin, J.N.H. Reek, Pd12MnL24 (for n = 6, 8, 12) nanospheres by post-assembly modification of Pd12L24 spheres, Chemical Science 14 (2023) 11840-11849.
[2] K. Keller, I. Ritsch, H. Hintz, M. Hülsmann, M. Qi, F.D. Breitgoff, D. Klose, Y. Polyhach, M. Yulikov, A. Godt, G. Jeschke, Accessing distributions of exchange and dipolar couplings in stiff molecular rulers with Cu(II) centres, Phys Chem Chem Phys 22(38) (2020) 21707-21730.
[3] A.M. Bowen, M.W. Jones, J.E. Lovett, T.G. Gaule, M.J. McPherson, J.R. Dilworth, C.R. Timmel, J.R. Harmer, Exploiting orientation-selective DEER: determining molecular structure in systems containing Cu(ii) centres, Physical Chemistry Chemical Physics 18(8) (2016) 5981-5994.
[4] B.E. Bode, J. Plackmeyer, T.F. Prisner, O. Schiemann, PELDOR Measurements on a Nitroxide-Labeled Cu(II) Porphyrin: Orientation Selection, Spin-Density Distribution, and Conformational Flexibility, The Journal of Physical Chemistry A 112(23) (2008) 5064-5073.
[5] T.F. Prisner, A. Marko, S.T. Sigurdsson, Conformational dynamics of nucleic acid molecules studied by PELDOR spectroscopy with rigid spin labels, Journal of Magnetic Resonance 252 (2015) 187-198.
[6] A.M. Bowen, C.E. Tait, C.R. Timmel, J.R. Harmer, Orientation-Selective DEER Using Rigid Spin Labels, Cofactors, Metals, and Clusters, in: C.R. Timmel, J.R. Harmer (Eds.), Structural Information from Spin-Labels and Intrinsic Paramagnetic Centres in the Biosciences, Springer Berlin Heidelberg, Berlin, Heidelberg, 2013, pp. 283-327.
[7] J. Keeley, T. Choudhury, L. Galazzo, E. Bordignon, A. Feintuch, D. Goldfarb, H. Russell, M.J. Taylor, J.E. Lovett, A. Eggeling, L. Fábregas Ibáñez, K. Keller, M. Yulikov, G. Jeschke, I. Kuprov, Neural networks in pulsed dipolar spectroscopy: A practical guide, Journal of Magnetic Resonance 338 (2022) 107186.
[8] S.G. Worswick, J.A. Spencer, G. Jeschke, I. Kuprov, Deep neural network processing of DEER data, Science Advances 4(8) eaat5218.